Collisional stripping of the rock mantle on the differentiated asteroid. K. Kurosaki[1] and M. Arakawa[2], [1]Kobe University (kenji.kurosaki@people.kobe-u.ac.jp) for first author, [2]Kobe University.

Introduction: The impact event on asteroids is important to consider the mass of debris [1,2,3], which causes the production of many kinds of meteorites. Especially, the origin of the iron meteorites is thought to be post-impact debris on a differentiated asteroid, such as 4 Vesta. The iron-rich rabble pile meteorite is thought to be the M-type asteroid such as 16 Psyche, which is formed from the differentiated asteroid that loses the rock mantle by the impact event. The origin of iron meteorites is an essential material for the formation history of objects with large iron cores, such as Mercury. That is, the origin of iron meteorites is important to consider the origin of planetary cores. The formation of the differentiated asteroid indicates the distribution of the material in the protoplanetary disk. The differentiated asteroid is thought to have been formed by heating radiatively decayed elements such as ^{26}Al. After the asteroid is differentiated, iron meteorites are formed by the impact when the differentiated body loses its rock mantle and iron core. However, impact event on the differentiated asteroid is not quite known. In this study, we perform the impact simulation for the differentiated asteroid to determine the escaping mass of the rock mantle and the iron core for various iron mass fraction.

Method: In this study, we performed numerical simulations of the impact event on differentiated asteroids using the standard SPH method. The standard SPH method is widely used for astronomical collisions [1,3,4]. In this study, we perform collision calculations for a differentiated source, such as Vesta, and discuss the amount of rock mantle and iron core ejection. The target is assumed to have an iron core surrounded by a rock mantle. The rock and iron equation of states are used for Tillotson EOS for the basalt and the iron, respectively [4]. The target mass is 10^{23} g. The impactor is the same as the target. This study ignores the cohesion and shear strength. The mass ratios of the iron cores were assumed to be 100%, 70%, 50%, 30%, and 0%. Impact velocities (V_{imp}) are 0.05 km/s-10 km/s. Head-on collisions are considered. The specific impact energy Q_R = 1/2 μ V_{imp}/M_{tot} where μ is the reduced mass [2]. We investigate the catastrophic disruption energy of the whole body and the rock mantle. Escaping particles for rock and iron are determined by their velocities whose velocities are faster than the escape velocity that is calculated by the gravitational potential from the largest remnant.

Results: We calculated the Impact simulation for to consider the catastrophic disruption threshold. We

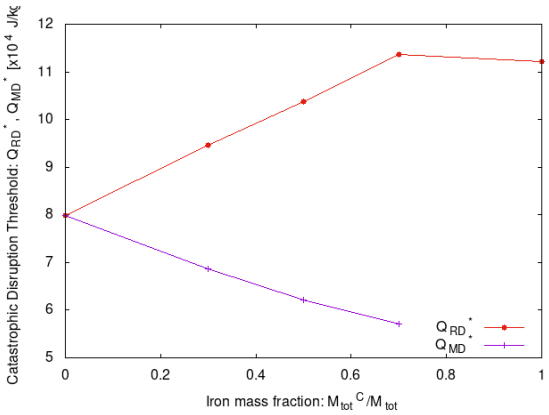

Fig 1. The catastrophic disruption threshold for various iron mass fraction of the target. Red line is Q_{RD}^*. The purple line is Q_{MD}^*.

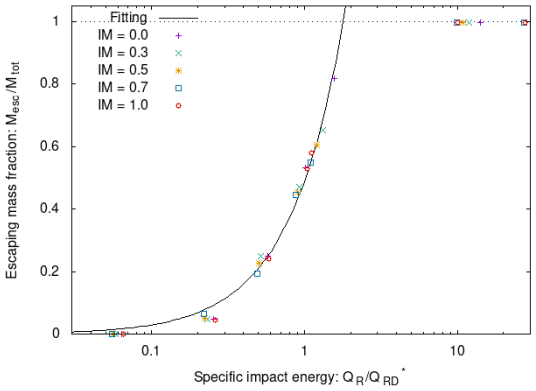

investigate the total escaping mass (M_{esc}), the escaping

Fig 2. The relationship between the escaping mass fraction and the specific impact energy normalized by Q_{RD}^*. Colors represents the iron mass fraction of the target (IM). IMs for purple points are 0.0 (pure rock), green points are 0.3, orange points are 0.5, blue points are 0.7, and red points are 1.0 (pure iron). The black line is the liner fitting as shown in Eq. (1).

mass of rock mantle (M_{ej}^M), and the escaping mass of iron core (M_{ej}^C). The catastrophic disruption threshold value is determined by interpolation between different simulations spanning a range of Q_R chosen to yield the escaping mass fraction is equal to 0.5. We investigated two kinds of the threshold. Q_{RD}^* is the threshold value for the total escaping mass fraction (f_{esc}= M_{esc}/M_{tot}), while Q_{MD}^* is the escaping rock mantle mass fraction (f_{esc}^R=M_{ej}^R/M_{tot}^R). Figure 1 shows Q_{RD}^* and Q_{MD}^* values for iron mass fraction (M_{tot}^C/M_{tot}). We find that

Q_{RD}^* increases as the iron mass fraction increases, while the Q_{MD}^* decreases, which means the rock mantle is easy to escape by the impact as the rock mantle mass decreases. Figure 2 shows the relationship between the escaping mass fraction and the specific impact energy. We find that the escaping mass fraction is shown by the power law fitting

$$f_{esc} = 0.49\ \bar{Q}^{1.2} \quad (1)$$

where $\bar{Q}$=Q_R/Q_{RD}^*. Our calculation showed the target and the impactor are catastrophic disruption in the case of $\bar{Q} \geq 10$, which is equivalent to $V_{imp} > 3$ km/s. The total escaping mass is composed of the sum of the escaping rock mantle (M_{ej}^R) and iron core (M_{ej}^C). Figure 3 shows the relationship between the escaping mass fraction and the specific impact energy normalized by Q_{MD}^*. Although the escaping mass increases with increasing the specific impact energy, only the rock mantle is ejected while the escaping mass of iron core is less than rock mantle. The escaping of the iron core occurs when the half of the mass of rock mantle has been escaped. We find that the escaping rock mantle is shown by the power law fitting

$$f_{esc}^R = 0.45\ \overline{Q_M}^{0.9} \quad (2)$$

where $\overline{Q_M}$=Q_R/Q_{MD}^*. Our results showed that the iron core begins to escape when $\overline{Q_M} \geq 1$. Moreover, the iron mass fraction of the largest remnant body increases when $\overline{Q_M} \leq 1$ because the iron core hardly escapes. Thus, the differentiated asteroid loses the rocky mantle prior to the iron core, which is the same phenomena for the impact simulation on the planet with the atmosphere [6]. In the case of destructive impacts, the iron core outflow is essential for forming iron-rock rubble pile bodies. However, the preferential destruction of the rock mantle suggests that iron-rich small bodies are more likely to form.

Discussion: M-type asteroids are considered to be iron-rich asteroids. Our study showed that the iron cores of the differentiated asteroids are likely to remain, while the rock mantle preferentially lose by the impact event. Our result also suggest that the differentiated asteroid's iron mass fraction will increase when the differentiated asteroids formed from rocky planetesimals undergo collisional mergers. However, the rock mantle fragments scattered by the collision may reaccrete on the post-impact asteroid because orbits of fragments formed by the rock mantle are close to the post-impact asteroid. If the rock fragments reaccretes on the post-impact asteroid, the asteroid's iron mass fraction does not increase. However, the time scale of the fragments' orbital motions is longer than the impact time scale and beyond the scope of this study.

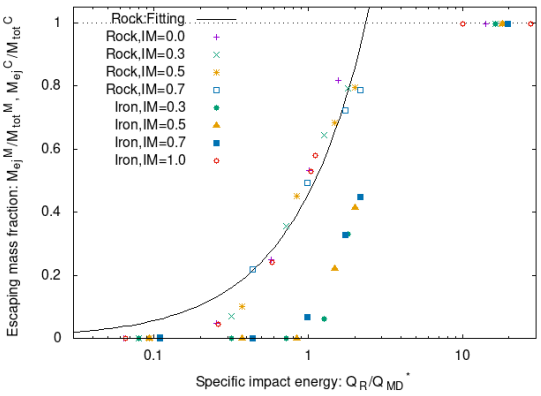

Fig 3. The relationship between the escaping mantle rock (crosses, x, asterisks, and open squares) and iron core (filled circles, filled triangles, filled squares, and open circles) fraction and the specific impact energy normalized by Q_{MD}^*. Colors represents the iron mass fraction of the target (IM), which is the same as Fig. 1. The black line is the liner fitting for escaping rock as shown in Eq. (2).

Conclusion: We performed the impact simulation on a differentiated asteroid to investigate the catastrophic disruption threshold and the escaping mass for various iron mass fraction by the smoothed particle hydrodynamics simulation. The total escaping mass can be represented by the specific impact energy normalized by Q_{RD}^*. On the other hand, the escaping mantle rock or iron core mass fraction can be normalized Q_{MD}^*. The iron core begins to escaping when Q_R is larger than Q_{MD}^* because the rocky mantle prevents the escaping of the iron core. Our finding suggests that the impact phenomena on the differentiated asteroid remains the iron core selectively.

Acknowledgments: Numerical computations were carried out on Cray XC50 at the Center for Computational Astrophysics, National Astronomical Observatory of Japan. This work is supported by JSPS Grants-in-Aids for Scientific Research No. 20J01258 (K.K.), 21H00039 (K.K.), 22H00179 (M.A.)

References: [1] Benz, W. & Asphaug, E. (1999), *Icarus, 142*, 5. [2] Leinhardt, Z. M. & Stewart, S. T. (2012), *ApJ, 745*, 79. [3] Genda, H., Fujita, T., Kobayashi, H., et al. (2017), *Icarus, 294*, 234. [4] Monaghan, J. J. (1992), *ARAA, 30*, 543. [5] Melosh, H. J. (1989), New York: Oxford University Press; Oxford: Clarendon Press, 1989. [6] Denman, T. R., Leinhardt, Z. M., Carter, P. J., et al. (2020), *MNRAS, 496*, 1166.